Developments in the Built Environment 17 (2024) 100368

Contents lists available at ScienceDirect

Developments in the Built Environment

journal homepage: www.sciencedirect.com/journal/developments-in-the-built-environment

Optimisation of mechanical properties and impact resistance of basalt fibre reinforced concrete containing silica fume: Experimental and response surface assessment

Idris Ahmed Ja'e [a,c,*], Raja Amirul Naquib bin Raja Sazrin [b], Agusril Syamsir [a,b,**], Naraindas Bheel [d], Chiemela Victor Amaechi [a,e], Teh Hee Min [d], Vivi Anggraini [f]

[a] Institute of Energy Infrastructure, Universiti Tenaga Nasional, Putrajaya Campus, Jalan IKRAM-UNITEN, 43000, Kajang, Selangor, Malaysia
[b] Department of Civil Engineering, Universiti Tenaga Nasional, Putrajaya Campus, Jalan IKRAM-UNITEN, 43000, Kajang, Selangor, Malaysia
[c] Department of Civil Engineering, Ahmadu Bello University, Zaria, 810107, Nigeria
[d] Department of Civil and Environmental Engineering, Universiti Teknologi PETRONAS, Seri Iskandar, 32610, Malaysia
[e] Engineering Department, Lancaster University, Lancaster, LA1 4YR, UK
[f] Civil Engineering Department, School of Engineering, Monash University Malaysia, Jalan Lagoon Selatan, Bandar Sunway, 47500, Selangor, Malaysia

ARTICLE INFO

Keywords:
Basalt fibre
Silica fume
Mechanical properties
Energy
Impact resistance

ABSTRACT

Although Basalt fibre reinforced concrete (BFRC) has a proven record of outstanding behaviour, concerns regarding the decline in its performance beyond certain content remains a major concern. To address this concern, a varying content of Silica Fume (SF) was introduced into the BFRC mix, and their combined influence on concrete's mechanical and impact resistance was investigated using experimental and Response Surface Analysis (RSA). Using regression models developed from experimental results, 13 responses of statistically designed experiments were predicted. The findings revealed significant improvement in the concrete performance with increases between 28% and 65% in compressive strength, 35%–107% in split tensile strength, 11%–46% in flexural strength and 117%–150% in the impact resistance. Therefore, appropriate proportions of BF and SF can be utilised as an eco-friendly sustainable material in concrete.

1. Introduction

Over the years, the goal of minimizing the environmental impact and carbon footprint associated with concrete production and utilisation, while simultaneously enhancing its mechanical performance and durability has evolved into a multifaceted approach. This involves the incorporation of a range of alternative sustainable materials including recycled waste, natural and synthetic fibres, fly ash, slag, glass, etc in the concrete production process. Depending on the intended application, these materials are introduced to either improve the mechanical characteristics, lower the embodied energy and carbon emissions, reduce waste generation, or extend the structural lifespan (Abbass et al., 2018; Lee et al., 2017; Sulaiman et al., 2020; Özkılıç et al., 2023).

Despite these efforts, normal concrete remains susceptible to crack-related problems in both its plastic and hardened state. Plastic cracks are the early-state microscopic fissures that develop from intrinsic stresses resulting from concrete settlement and shrinkage within the first 24 h after being cast. The long-term cracks appear due to shrinking afterwards. To address these issues and improve concrete toughness for structural applications, the incorporation of natural and synthetic fibres in concrete has propelled the advancement in fibre-reinforced concrete technology. Different fibres of varying sizes and moduli of elasticity have been incorporated into concrete to enhance its mechanical characteristics by minimizing shrinkage-cracking propagation.

* Corresponding author. Institute of Energy Infrastructure, Universiti Tenaga Nasional, Putrajaya Campus, Jalan IKRAM-UNITEN, 43000, Kajang, Selangor, Malaysia.
** Corresponding author. Institute of Energy Infrastructure, Universiti Tenaga Nasional, Putrajaya Campus, Jalan IKRAM-UNITEN, 43000, Kajang, Selangor, Malaysia.
E-mail addresses: Idris.ahmad@uniten.edu.my (I.A. Ja'e), rajaamirulnaquib@gmail.com (R.A.N. Raja Sazrin), Agusril@uniten.edu.my (A. Syamsir), naraindas04@gmail.com (N. Bheel), chiemela.victor@uniten.edu.my (C.V. Amaechi), heemin.teh@utp.edu.my (T.H. Min), vivi.anggraini@monash.edu (V. Anggraini).

https://doi.org/10.1016/j.dibe.2024.100368
Received 25 November 2023; Received in revised form 11 February 2024; Accepted 11 February 2024
Available online 17 February 2024

The application of fibre-reinforced concrete is widely recognised and still evolving due to its enhanced post-cracking tensile strength, resulting from the reinforcing mechanism developed by the fibre within the concrete matrix. For the construction of energy infrastructures, and other structural purposes where high-performance concrete is required, the utilisation of natural and synthetic fibres separately and in hybrid form is extensively being investigated to improve the ductile performance of conventional concrete. Several studies have investigated the inclusion of basalt, kenaf (Jae et al., 2023), polypropylene, steel fibres (Atea, 2019), and other fibrous materials (Bheel et al., 2023) separately with a positive influence on concrete ductility, toughness, flexural, split tensile strength and impact resistance while effectively controlling the proliferation of microcracks (Banthia and Sappakittipakorn, 2007).

Over the years the utilisation of fibrous material has evolved beyond Fiber reinforced concrete to the enhancement of other concrete types such as engineered cementitious composites (Bheel et al., 2023), Self-compacting concrete (Zhang et al., 2022), and even in hybrid form for structural retrofitting. Basalt fibre, in particular, has gained research attention for its numerous advantages, such as mechanical properties, durability, physicochemical properties, low energy consumption, economic production process, strength and enhanced resistance to alkaline, acidic and salt attack compared to other fibrous materials. As a product of basalt rock, it is manufactured by melting crushed basalt rock and melting it to around 1500 ^{O}C and extruding it through small nozzles to produce a continuous filament of Basalt Fibres (BF). Being a mineral fibre, BF is not decomposable and poses no threat to the environment (Li et al., 2022a). It is characterised by high elastic modulus, high fracture strength, superior frost, and corrosion resistance. Its density is similar to ordinary cement, making it advantageous for providing better bonds with improved mechanical properties. In terms of tensile strength and elastic modulus, BF ranges between 3000 and 4500 MPa and 80–100 GPa respectively, outperforming aramid fibre, polyethene fibre, and polypropylene (Scalici et al., 2016) and offers an economic advantage in terms of manufacturing process and availability in large quantities.

Apart from being a mineral fibre, basalt fibre has a density similar to that of ordinary Portland cement. Its high elastic modulus affords it the ability to establish better bonds with improved mechanical properties. Accordingly, the reinforcing efficiency is contingent on the improved fibre-matrix interfacial properties. This has been demonstrated by pull-out tests which have revealed the average bonding strength is more effective than the equivalent shear bonding strength. Moreover, the bonding strength can be improved with increased fibre length.

Thus, leveraging its excellent characteristics, several studies have explored the use of basalt fibre-reinforced concrete. For instance, one study examined the effect of chopped basalt fibre on the workability, compressive strength, and impact resistance of high-performance concrete (HPC) using an empirical model to study the relationship between impact energy and compressive strengths. The study used fibre lengths of 3 mm, 12 mm and 18 mm and volume fractions of 0.075%–0.6%. The findings showed an improvement in compressive strength from 12.2% to 17.5% and an enhancement in the impact resistance due to the enhancement in the microstructure (Tahwia et al., 2023). Another study examined the effect of water binder ratio, fibre volume fraction, fibre length, and fly ash content on the mechanical properties of basalt fibre self-compacting high-strength concrete with the results indicating that the water binder ratio had the most significant impact on compressive strength Meanwhile, fibre volume fraction and length were found to influence improvements in compressive and flexural strengths, crack resistance, and toughness (Xue et al., 2023). Similarly, an experimental study on flexural loading on Basalt Fibre Reinforced Concrete (BFRC) reveals a significant increase in the tensile strength, cracking load, ultimate load carrying capacity, reduced propagation of cracks and reduced permeability at an optimal content of 0.3% (Philip et al., 2023). Several studies have reported similar improvements in concrete performance at varying volume fractions of basalt fibre (Wu et al., 2023; Xie et al., 2023).

Other studies have explored the potential benefits of incorporating silica fume into basalt fibre-reinforced concrete, with a particular focus on its influence on concrete workability, strength and durability of concrete. However, it is worth noting that depending on the introduced content it can lead to an increase in brittleness of the concrete (Köksal et al., 2022; Adil et al., 2020). Furthermore, researchers have also explored the contributions of other pozzolanic materials (IA et al., 2019). Silica Fume (SF) as a byproduct of the production of silicon is classified as a very reactive pozzolanic material consisting of very fine particles of silicon dioxide which enhance its mechanical properties. Adding SF to the concrete mix provides improved pore densification, reduced CO_2 emission, enhanced compressive and tensile properties, durability and permeability and chloride penetration thereby protecting steel reinforcement against corrosion. However, beyond certain content, a resulting adverse effect may occur due to the dilution of cement. Depending on the applications, different silica foam content has been reported for the best performance. For instance, 5% has been documented as the optimum content for pervious concrete (Adil et al., 2020), 15% in high-strength concrete and 16–20% in silica fume self-compacting concrete (E Taha et al., 2019).

The addition of silica fume has been shown to improve the mechanical properties of basalt fibre-reinforced concrete. This finding has led to the development of highly durable and lightweight insulating foam concrete with a compressive strength of up to 46 MPa, as well as an enhanced pore network and fibre-paste matrix. By evaluating the concrete's physico-mechanical, thermos-durability, and insulation properties of the foam concretes the effect of the basalt fibre was observed to be more dependent on the use of silica fume, potentially due to its low integration with cementitious paste. Samples with 15% silica fume saw a specific increase of up to 46% in compressive strength, although with increased brittleness compared to samples without silica fume. Moreover, samples with 0%–3% basalt fibre experience an increase in flexural strength of up to 88% (Gencel et al., 2022). Experimental and numerical assessments also revealed an improvement in the mechanical strength of lightweight basalt fibre-reinforced concrete containing silica fume and fly ash (Saradar et al., 2020). This finding further highlighted a reduction in shrinkage with 1.5% fibre volume. Furthermore, the experimental program investigated the physical, mechanical and durability performance of high-strength mortar with basalt fibre and silica fume at ambient and elevated temperatures and curing regimes. However, a partial replacement of 10% of silica fume was considered for cement with varying basalt fibre between 0% and 0.6%. An improvement in compressive strength (up to a maximum of 31%) at ambient temperature was observed with a corresponding reduction in flowability with each increase in basalt content (Koksal et al., 2021).

Based on the literature search conducted, previous studies on basalt fibres and silica fume are mostly focused on individual influence on mechanical properties of mortar, foam concrete and lightweight concrete. This limited scope fails to account for the complex concrete properties consisting of multiple variables as highlighted in (Emad et al., 2022) and particularly negates the goal of determining a combined optimal volume fraction for multiple responses. Thus, this study aims to fill this gap by investigating the combined impact of basalt fibre and silica fume on concrete's mechanical and impact resistance and also investigate the optimised volume fractions using experimental and response surface methodology (RSM). The outcome of this study will be relevant in facilitating a better understanding of the synergistic influence and optimization of varying dosages of basalt fibres and silica fume for specific structural applications where resistance and durability, improved mechanical properties and cost-effectiveness, and sustainability are primary factors of consideration.

For ease of reference, the paper is structured in the following order: section one covers the introduction, while section two details the materials, concrete mix design and test procedure. Section three presents the Response Surface Analysis and Optimization of Basalt fibre and Silica fume content for optimal responses, while sections four and five

contain the results and discussions, and graphical optimization respectively. The final section contains the conclusions.

2. Materials, Concrete mix design and Test procedure

2.1. Materials

To produce plain concrete, Ordinary Portland cement (OPC), potable water, fine and coarse aggregates in the range 5–10 mm and 10 mm–20 mm respectively were utilised. For Basalt fibre-reinforced concrete, the same ingredients along with BF and SF were used. Superplasticizer (SP: Master Gienium ACE 8522) was used in BFRC to enhance its workability. Silica Fume (SF) and SP were purchased from local suppliers, in Malaysia while BF was imported from China. The BF sample in strips of 50 mm in length and an approximate diameter of 0.62 mm was used to produce a homogeneous mixture as shown in Fig. 1.

The physical characteristics of the basalt fibre used are presented in Table 1.

The oxide composition of the OPC and silica fume as determined using X-ray Fluorescence Spectroscopy (XRF) is shown in Table 2.

2.2. Concrete mix design

In the experimental investigation, four concrete mixes consisting of one control sample (CS) and three with basalt fibre (BF) and silica fume (SF) were prepared for the experimental investigation. The CS is a normal concrete made of 450 kg of cement, 1755 kg of aggregate, and a water-cement ratio (W/C) of 0.40. The specimen samples containing basalt and silica fume were prepared using three fibre volume fractions of 0.5%, 1.0%, and 1.5%, consisting of 1%–5% dosage each of SF by weight of cement. In each case, the SF was added a few minutes after adding water, while BF was introduced after the concrete mixture was ready. The mixture was remixed for 5 min to ensure even distribution in the concrete mix as shown in Fig. 1(c). A reduction in the mix workability was observed with increased BF content. This is attributed to several factors such as increased fibre surface area, which absorbs excess hydration water resulting in increased concrete viscosity causing it to agglomerate around the fibres (Mazloom et al., 2020; Mazloom and Mirzamohammadi, 2021). Furthermore, the fibre's high aspect ratio can lead to clustering causing resistance to concrete flow (Adesina et al., 2020; Mazloom and Mirzamohammadi, 2019; Abna and Mazloom, 2022). The concrete mixes containing basalt fibre and silica fume are represented by the nomenclatures; BFRC-0.5%, BFRC-1.0%, and BFRC-1.5% as shown in Table 3.

A total of 48 concrete samples were prepared, three each for compressive, split tensile, flexural and impact resistance and tested at 28 days of curing age. Table 4 summarizes the sample shapes and dimensions used. Each sample was prepared in three layers, each layer vibrated for 15–20 s on the vibrating table to expel trapped air. Excess concrete was removed and the upper surface was levelled and allowed to

Table 1
Physical properties of Basalt fibre.

Property	Dimension
Diameter (mm)	62
Length (mm)	50
Density (g/cm^3)	2.65
Tensile strength (MPa)	3800
Elastic Modulus (GPa)	97
Ultimate Elongation (%)	2.8

Table 2
Chemical composition of OPC and silica fume.

Oxides	Composition (%)	
	Cement	Silica Fume
Lime (CaO)	64.54	1.85
Silica (SiO_2)	21.28	92.9
Alumina (Al_2O_3)	5.60	0.16
Sulphur Trioxide (SO_3)	2.14	–
Magnesia (MgO)	2.06	0.25
Iron Oxide (Fe_2O_3)	2.36	0.59
Alkalies (K_2O, Na_2O)	0.44	1.04
P_2O_5	0.17	–
TiO_5	0.51	–
Loss of Ignition (LOI)	0.64	0.3

Table 3
Concrete mix design for experimental investigation.

Mix design	CS	BFRC-0.5%	BFRC-1.0%	BFRC-1.5%
Cement (kg)	450	450	450	450
W/C	0.40	0.40	0.40	0.40
Aggregate (kg)	1775	1775	1775	1775
BF content (%)	0	0.5	1.0	1.5
SF dosage (%)	0	5	5	5

Table 4
Detail of samples used for experimental tests.

Tests	Sample shape and dimension (mm)		No. of samples	Curing age	Reference standard
Compressive strength	Cube	100 x 100 x 100	12	28 days	ASTM C109/ C109 M
Split tensile strength	Cylinder	150 x 300	12	28 days	ASTM C496/ C496 M
Flexural strength	Prism	500 x 100 x 100	12	28 days	ASTM C293/ C293 M
Impact resistance	Cylinder	75 x 150	12	28 days	ASTM D1557

Fig. 1. Sample illustration of (a) Basalt fibre (b) Silica fume (c) Basalt fibre concrete mix.

set at room temperature. Samples were de-moulded after 24 h and cured in a water bath at 22 °C with 100% relative humidity for 28 days. The stress-strain behaviours of the samples are explicitly explored (Bhonde et al., 2022).

2.3. Test procedure

2.3.1. Compressive strength test

Compressive strength test was performed using the Universal Testing Machine (UTM) available at the civil engineering department of Universiti Tenaga Nasional, Malaysia. The test was conducted under uniaxial compressive force following ASTM C109/C109M-02. The result of each load and displacement was recorded through a data logger.

2.3.2. Split tensile strength test

The split tensile strength test was conducted using the same UTM in section 2.2 in accordance with ASTM C496 C496/C496M − 17, 2011. Each cured sample was air-dried and weighed and the edge was marked with pivoted lines to ensure proper alignment of the sample axis. Specimen centrally positioned on a bearing available on the UTM board, thereafter the machine's upper crosshead was lowered gradually to ensure contact with the specimen. Thereafter, loading was gradually applied in the range of 0.7 MPa/min to 1.4 MPa/min until the sample failed.

2.3.3. Flexural strength test

The flexural test was performed using the three-point loading test in accordance with ASTM C293/C293 M, 2022. Each specimen was properly horizontally positioned, and the LVDTs fitted to the record, the load was gradually applied at 0.2 mm/min from the upper central part until failure.

2.3.4. Impact resistance test

The impact resistance of concrete samples from each concrete mix was tested by sequentially dropping an 8.5 kg weight through a height of 63 mm on each of the 150 mm × 75 mm samples, and repeatedly until failure. The number of blows at which the first crack appears was recorded.

3. Response Surface Analysis and Optimization of Basalt Fibre and Silica Fume content for optimal responses

3.1. Response surface analysis

More often, theoretical models that correlate the relationship between multi-variables (factors) and responses for specific systems are either not available or are complex. Such correlations are mostly not explicitly highlighted by the experimental approach. Hence, empirical methods such as Response Surface Methodology (RSM) are utilised (Sarabia et al., 2009).

As a globalized technique, the RSM is an excellent empirical tool whose application includes the development of mathematical models for the prediction of correlational influences between multiple responses and factors, the generation of statistical design of experiments and the determination of optimum mix proportions by establishing targets for both responses and factors. Thus, Response Surface Analysis (RSA) involves the application of mathematical and statistical approaches in the modelling and analysis of problems where the main interest is to examine the influence of component variables on the responses of a system. The interactions between variables are represented graphically (response surface) to illustrate how each response(s) is influenced by the variation of individual or multiple variables. The RSA is implemented using several tools including Minitab and design expert software. Several researchers have utilised this technique for optimising factors in an experiment (Poorarbabi et al., 2020; Abdulkadir et al., 2021; Khan et al., 2023). In this study, the latter, Design-Expert V13:2021 was adopted because of its versatility.

The randomised optimal (custom) design model was adopted for its flexible design structure to accommodate custom models. The mix proportions of the factors (Basalt fibre and silica fume) were generated using upper and lower limits volume fractions of 0.5% 1.5%; 4% and 5% respectively. Using the regression models developed from experimental results, responses of statistically designed experiments were predicted and analysed using linear regression with no model transformation considered.

For each response (compressive, split tensile, flexural strength and impact resistance) a suitable model is suggested based on the level of significance (p-value) of each of the factors on the correlational relational relationship between the dependent (factors) and independent variables (responses). Depending on these relationships, a linear or polynomial response model is adopted as shown in equation (1) and (2).

$$f = \beta_0 + \beta_1 x_i + \beta_2 x_{ii} \ldots \beta_n x_n + \varphi \tag{1}$$

Where f and x represents the factor x and variable respectively. Also, β_0 is the intercept at $x_i = x_j = 0$, β is the coefficient.

$$f = \beta_0 + \sum_{i=1}^{n} \beta_i x_i + \sum_{i=1}^{n} \beta_{ii} {x_i}^2 + \sum_{i=1}^{n-1} \sum_{j>1}^{n} \beta_{ij} x_i x_j + \varphi \tag{2}$$

Where i and j denote linear and quadratic encrypted quantities, and n is the numerical variables.

The suitability of each model is validated using Analysis of Variance (ANOVA) and Fit statistics. The ANOVA describe the overall statistical significance and lack of fit of the model, while the fit statistics describe the *standard deviations*, and adjusted and predicted coefficient of determinations (R_a^2 *and* R_p^2). By determining the mean variability between the experimental and predicted mechanical properties and impact resistance, each model should have the required threshold expected to be statistically significant with a non-significant lack of fit, i.e., with corresponding $p - values\ of \geq 0.05$ and ≤ 0.05 respectively. The p-value indicates whether or not the suggested model is statistically significant.

On the other hand, the coefficient of determination measures how well the model fits the data. A high R^2 (close to 1) indicates how well fitted and that most of the variation in the dependent variable can be explained by the independent variable. An acceptable threshold of the difference between the adjusted coefficient (R_a^2) and the predicted (R_p^2) is less than 0.2 (Design Expert Software, 2021). Upon this validation, a diagnostic analysis of the correlation between the factors and responses is conducted to highlight the relationships between predicted and actual responses, number of runs and residuals, etc. Finally, the graphical representation of the model responses is generated and analysed.

3.2. Optimization of basalt fibre and silica fume for optimal responses

The optimum responses; that is the best-combined values of compressive strength, split tensile strength, flexural strength and impact resistance that can be achieved using a combination of factor levels (volume fraction of basalt fibre and silica fume) that simultaneously satisfy the criteria placed on each of the responses and factors. Model fit for each of the model responses used as optimization criteria has been determined through ANOVA while the range of the factors was automatically included.

The design evaluation was checked using ANOVA statistics, and diagnostics graphs to ensure the models provide a good estimate of the true response surface. The numerical optimization module in Design Expert software version 13.0 is based on a multi-response approach referred to as desirability. The approach utilises the desirability function as the objective function which reflects the desirable range of each response.

The graphical optimization approach module of the design expert software (version 13.0, 2022) was used to determine regions where

response requirements simultaneously meet the critical properties based on the defined ranges. For each response, a value equivalent to 30% higher than the control sample was defined as the lower limit while the highest predicted value was defined as the upper limit. The optimised response region is presented in the form of overlay contour plots.

4. Results and discussion

4.1. Response surface analysis

4.1.1. Regression models and predicted responses

Regression models used for the prediction of responses are developed from experimental results. Equations (1)–(4) represent models of compressive strength, split tensile strength, flexural strength and impact resistance of the samples respectively. The predicted responses are highlighted in Table 5 and will be discussed in tandem with the experimental results in the subsequent sections.

$$f_{C28} = 45.9 - 5.04\boldsymbol{BF} - 0.6794 * \boldsymbol{SF} \quad (1)$$

$$f_{Sts28} = 37.7037 + 32.9539 * \boldsymbol{BF} + 17.2677 * \boldsymbol{SF} - 0.6474 * \boldsymbol{BF} * \boldsymbol{SF} - 14.5157 * \boldsymbol{BF^2} - 1.9963 * \boldsymbol{SF^2} \quad (2)$$

$$f_{flx28} = 8.5650 + 1.1674 * \boldsymbol{BF} - 0.8067 * \boldsymbol{BF} \quad (3)$$

$$f_{IR28} = 22.118 - 16.4014 * \boldsymbol{BF} - 4.3993 * \boldsymbol{SF} + 5.3279 * \boldsymbol{BF} * \boldsymbol{SF} \quad (4)$$

Based on the ANOVA analysis performed on the actual regression models for all responses confirmed all models as significant, with p-values <0.05 and non-significant lack of fits (>0.05.) The differences between R^2_{adj} and R^2_{adj} in all models were consistently maintained at < 0.2, with adequate precision values > 4. These metrics fall within the acceptable limit of the Design Expert software version 13 utilised in this study.

4.2. Compressive strength

4.2.1. Experimental results

Based on compression test performed on twelve cubic samples, three for each of the four-mix designs (CS, BFRC-0.5%, BFRC-1.0% and BFRC-1.5%) the average compressive strength and stress-strain curve at 28 days are presented in Figures (2a) and (2b) respectively. A general increase in compressive strength is observed in samples containing basalt fibre, with the highest compressive strength of 46.5 MPa observed at 1% fibre content. However, as the fibre content increased from 1% to 1.5%, the strength decreased, possibly due to factors such as uneven distribution of fibre in the concrete matrix beyond 1% resulting in voids within the concrete structure (Bheel et al., 2023). The error bars in Fig. 2 (a) confirm the significance of the average results since no overlap is observed.

Table 5
Predicted mechanical properties with various Basalt fibre and Silica Fume.

Run	Factors (%)		Responses			
	Basalt Fiber	Silica Fume	Compressive Strength (MPa)	Split tensile Strength (MPa)	Flexural Strength (MPa)	Impact Resistance (blows)
1	0.17	3	49.03	1.04	6.35	8.85
2	0.5	1	46.70	−9.91	8.34	12.18
3	1	5	40.76	13.91	5.70	10.36
4	1.5	1	37.53	−6.63	9.51	1.11
5	0.95	3	41.90	12.49	7.25	8.52
6	0.95	3	41.90	12.49	7.25	8.52
7	0.95	5.83	40.93	9.75	4.97	10.40
8	0.95	0.17	42.86	−16.70	9.54	6.65
9	1.5	5	36.17	10.64	6.28	15.48
10	0.95	5	41.22	13.86	5.64	9.85
11	0.95	3	41.90	12.49	7.25	8.52
12	0.5	5	45.34	9.97	5.12	5.24
13	1.73	3	34.76	6.38	8.16	8.20

The stress-strain response plot depicted in Fig. 2(b) demonstrates a comparable initial behaviour for all samples, with BFRC-1.0% exhibiting a stiffer curve leading up to the peak stress. However, based on the strain values of 0.021 (CS), 0.022 (BFRC-0.5%), 0.020 (BFRC-1.0%) and 0.019 (BFRC-1.5%) corresponding to the maximum stress, the sample containing 0.5% basalt fibre (BFRC-0.5%) can be seen to withstand larger deformations before reaching maximum stress compared to other samples. Moreover, the normalised stress ratio plot indicates a gradual drop in ultimate stress in the post-plastic deformation phase. An increase in ultimate strain is also observed with an increase in fibre content, which is an indication of enhanced performance to undergo deformation beyond the initial cracking. Among all the samples, the BFRC-1.5% concrete exhibits the highest ultimate strain of 0.0317, which is about 13% higher than BFRC-1.0% and only about 6% higher than CS. Thus, depending on the intended application, each specimen presents a unique advantage in terms of strain at peak stress and ultimate strain.

Nonetheless, to further explore these relationships, plots of normalised stress ratio (NSR) with strain are compared in Fig. 2(c.). The linear elastic pattern of concrete samples can be seen to be similar across different loading before attaining peak strength. Subsequently, samples containing BF exhibit an enhanced ductile characteristic when compared to the control sample. Interestingly, the BFRC-1.5% concrete depicts a higher response from the onset and continues to exhibit the highest strain before failure. Thereby indicating that an increase in BF content leads to enhanced concrete ductility.

The general improvement in compressive strength and the overall stress-strain performance of samples containing basalt fibre and a single dose of silica fume is attributed to several factors such as the fibre's high tensile strength which allows it to distribute and support loads in the concrete matrix. Furthermore, the efficient distribution of the fibre reinforcement network in the concrete prevents the proliferation of cracks resulting in delayed failure. Moreover, the densification of pores between cement grain due to the presence of Silica Fume (SF) produced enhanced particle packing, with consequent increased overall strength. Thus, the improved bonding developed between the basalt fibre, silica fume and the cementitious matrix due to the combination of more calcium silicate hydrate gel with high tensile strength of the fibre enhances stress transmission from the concrete matrix to the fibre, thereby increasing the load-carrying capacity with effective load transfer, and minimal sliding or debonding of fibre, hence resulting in increased compressive strength.

4.2.2. Response surface results

To further examine the relationship of the basalt fibre-reinforced concrete (BRFC) samples with varying SF content, the predicted compressive responses presented in Table 5 are illustrated using 2-D contour and 3-D response surface plots as shown in Fig. 3 (a) and (b). From the figures, compressive strengths in the range of 38 MPa–47 MPa can be seen to be obtained within BF and SF values of 0.4%–0.62% and 1%–4% respectively.

The highest predicted value of 47.29 MPa (at 0.4%BF and 1%SF) shows a 65% increase compared to the control sample (28.76 MPa). The predicted results showed a general improvement of between 28% and 65% in compressive strength can be seen to be in close agreement with the experimental results, thus affirming the accuracy of the regression models. In addition, the response surface results provide a wide range of options in terms of combined fractions for improved ductility of the basalt fibre concrete.

Furthermore, the variation in SF content can be seen to slightly influence the output in that range. Nonetheless, the trend of strength development is consistent with the documented facts from the literature on the densification of the cementitious matrix and ITZ (Abdulkadir et al., 2021). In another study (Mazloom et al., 2004), a 21% increase in

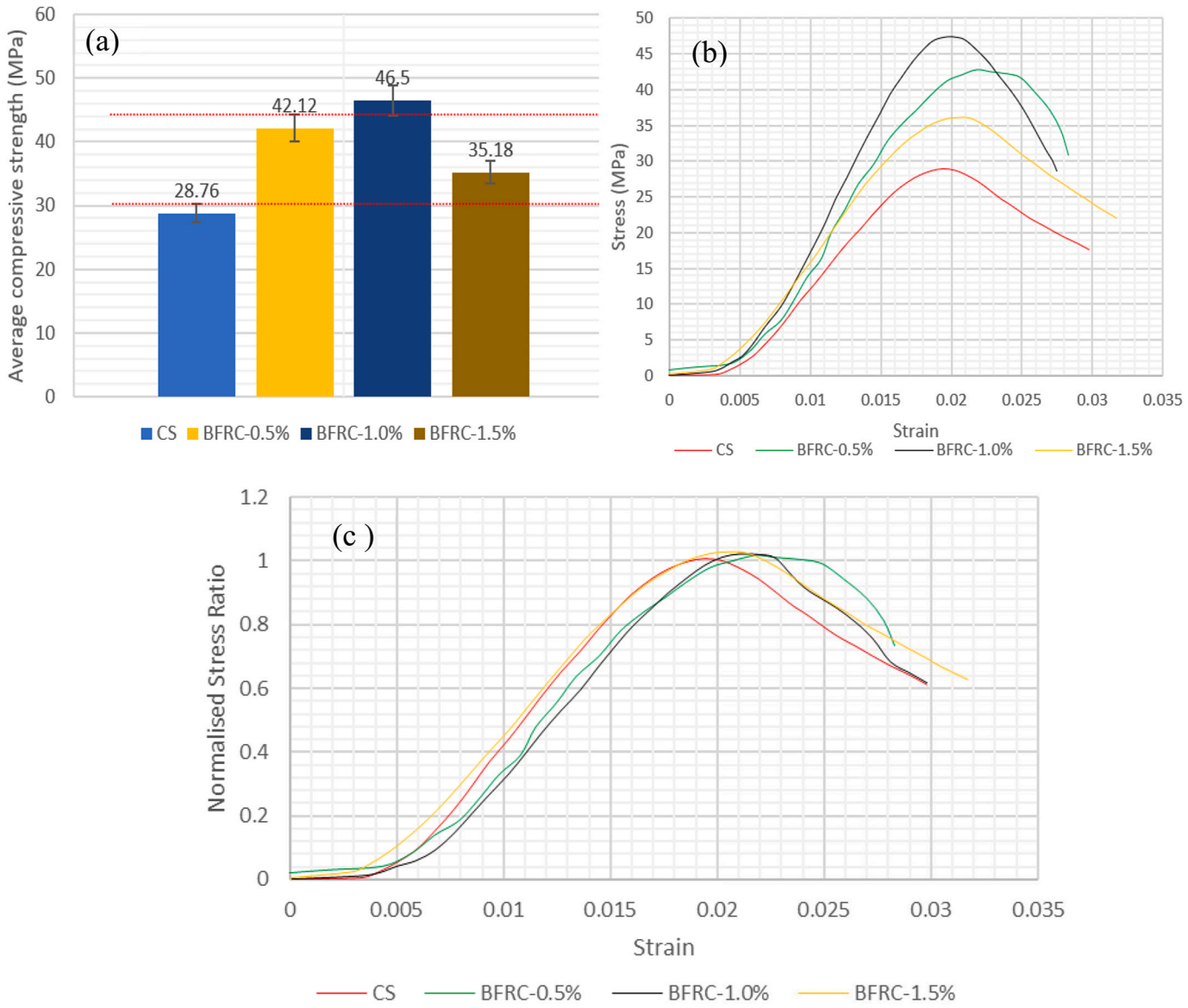

Fig. 2. BFRC Compressive results at 28 days (a) Compressive strength (b) Stress-Strain curves (c) Normalised stress ratio.

compressive strength with the addition of 15% SF in a normal curing condition. Albeit, other studies have reported a decrease in compressive strength with the addition of BF, with reported cases by up to 18% (Sadrmomtazi et al., 2018). A reduction of 27% has also been reported when BF over 1% volume fraction is used (Dias and Thaumaturgo, 2005). Nonetheless, several studies have reported improvement in compressive strength with the inclusion of BF content between 0.3% and 0.8% (ZIELINSKI and OLSZEWSKI, 2005). Thus, the result presented in Fig. 3 represents an improvement of the compressive strength with a reduced SF content due to the complemented performance of the BF.

4.3. Split tensile strength

4.3.1. Experimental results

The comparison of the average 28-day split tensile strength of cylindrical concrete samples containing different fractions of basalt fibres (BF) and constant dosage of silica fume is shown in Fig. 4(a). The results indicate that the tensile strengths of samples containing basalt fibre are notably higher than the control sample with the maximum values obtained in the sample containing 1% basalt fibre. Overall, the inclusion of 0.5%, 1.0% and 1.5% BF content yielded an improvement of 14.1%, 117% and 38.5% respectively.

To further explore the influence of the BF on the nonlinear behaviour of the basalt fibre-reinforced concrete after undergoing plastic deformation, the instantaneous modulus (IM) as a function of strain is computed and compared in Fig. 4(b). The IM otherwise known as tangent modulus is computed as a derivative of points on the stress-strain curve. The resulting plot offers valuable insight into the hardening and softening behaviour of the samples during deformation. It can be observed from the plot that the tangent modulus of CS, BFRC-0.5%, BFRC-1.0% and BFRC-1.5% gradually increases up to 10%, 21%, 35% and 15% of the strain corresponding to the ultimate stress respectively. Thereafter, the plot reflects the evolution of microcracks leading to the non-linearity of the samples until they reach ultimate stress and continue to soften until failure.

Based on the findings, it appears that the BFRC-1.0% concrete demonstrated a superior capability of withstanding loading for a longer duration before microcracks became apparent. The sample also displayed improved softening behaviour, meaning that even after microcracks developed, they did not regenerate as quickly as observed in other samples. Thus, considering this as well as the enhanced compressive performance, it could be argued that the BFRC-1.0%

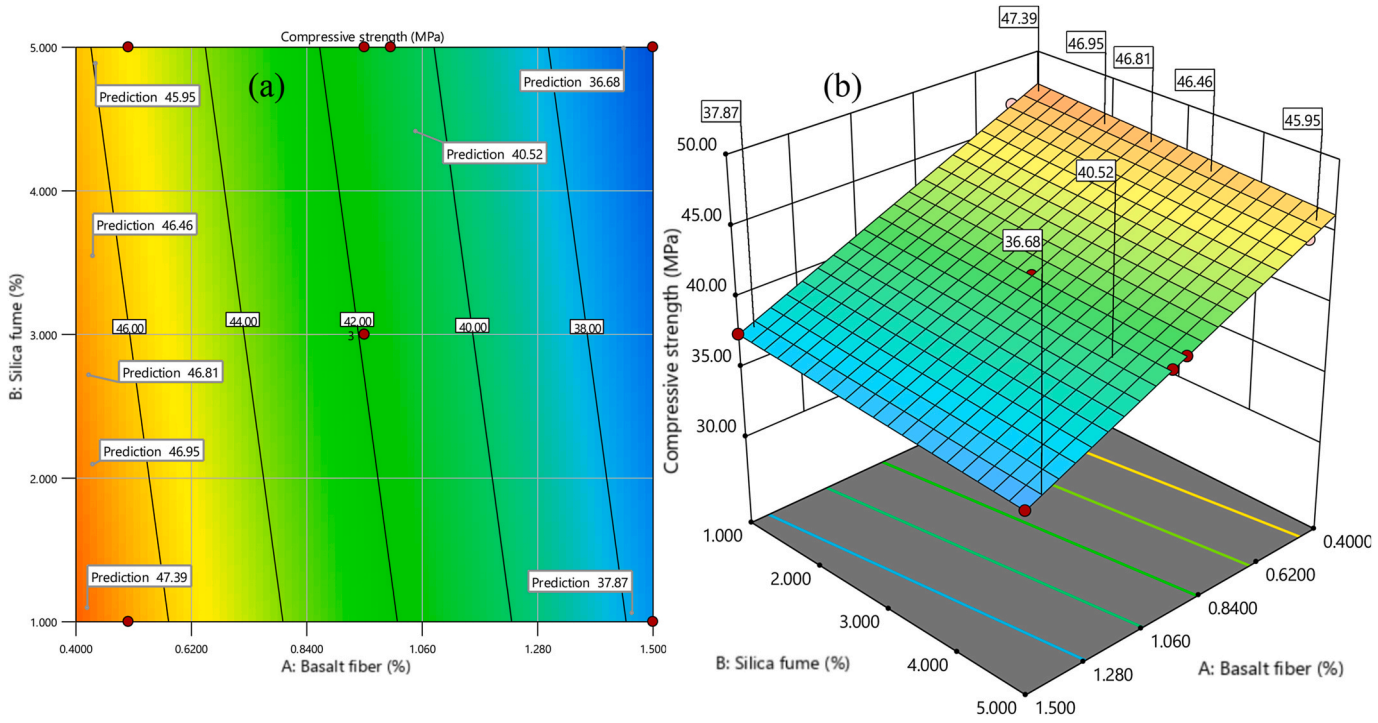

Fig. 3. (a) 2-D contour (a) 3-D response surface representation of the influence of Basalt fibre and Silica Fume on compressive strength of concrete.

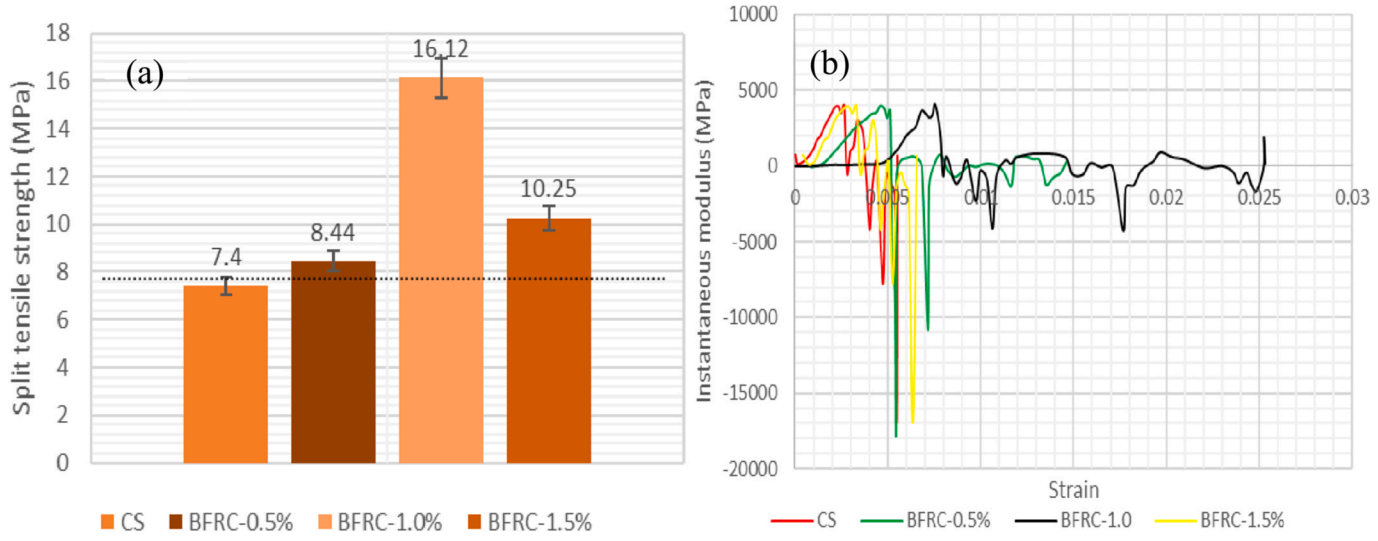

Fig. 4. (a) Average Split tensile strength of BFRC at 28 days (b) Instantaneous modulus of concrete specimens at varying loading regimes.

concrete represents the optimal choice.

4.3.2. *Response surface results*

Having examined the experimental results with a single dose of Silica Fume (SF), the response surface methodology is utilised to further investigate the combined influences of varying content of BF and SF on the split tensile strength of concrete samples. The responses are compared using a contour plot and a 3-D response plot in Fig. 5 (a) and (b) respectively. It can be observed from the contour plot that the addition of 2.8% SF and 0.5% BF content results in increased tensile strength above the control sample. Furthermore, the development of tensile strength is directly proportional to the increase in both SF and BF. In comparison to the control sample, it is worth noting that an increase of about 35%–107% in tensile strength can be observed with SF and BF in the range of 2.8%–5% and 0.4%–1.5% respectively. This provides a range of alternatives for various applications. Notably, the maximum split tensile strength of 15.22 MPa was achieved at 1% and 4.5% BF and SF respectively, which falls within the same range as the observed compressive strength.

Thus, it can be inferred here that the split tensile strength of concrete is enhanced by the addition of BF and SF due to the improved bond between the BF and C–S–H gel which facilitates an increase in the concrete's fracture energy, higher ultimate loading capacity and energy absorption as evidently illustrated in Fig. 5(b). Similar findings have been reported in several studies. For example, Jiang et al., (Sadrmomtazi et al., 2018) showed 14%–24% with the inclusion of BF.

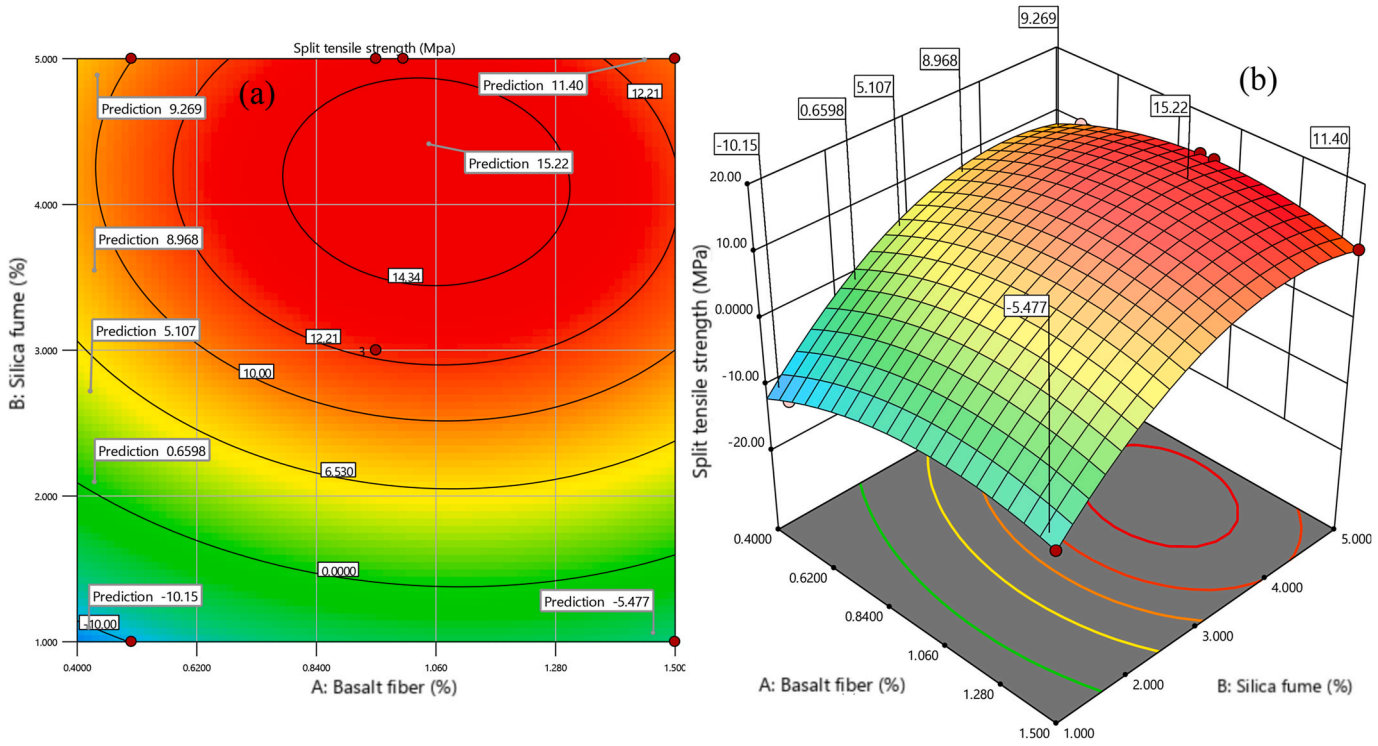

Fig. 5. (a) 2-D contour (b) 3-D response surface representation of the combined influence of Basalt Fiber and Silica Fume on Split tensile strength.

4.4. Flexural strength

4.4.1. Experimental results

In Fig. 6, the flexural strength of concrete samples containing varying fractions of basalt fibre (BF) and silica fume (SF) is compared. The results showed a consistent improvement in flexural strength between 4.3% and 14.8% as the BF content increased. The highest strength observed was 6.44 MPa at 1.5% BF content which demonstrates improved resistance to tensile stresses and evolution of significant cracks. However, when compared with the improvement in compressive strength, modulus of elasticity and split tensile strength, the flexural results did not show significant improvement. The only realistic reason for the low improvement could be due to the fibre length (50 mm) considered.

Nonetheless, the improvement observed is attributed to the synergistic effect of the BF with SF resulting in an enhanced fibre-paste matrix. This consequently enhances the energy absorption and flexural ability of the concrete. This is indicated by the improved properties in samples with higher fibre content as observed in the failure modes illustrated in Fig. 7 through the gradual reduction in crack width after failure.

Furthermore, the inclusion of silica fume increased the production of extra calcium silicate hydrate (C–S–H) gel, leading to the development of more robust cementitious linkages and ultimately improving the concrete's flexural strength. This increased ductility is particularly advantageous for applications where the concrete is exposed to dynamic loading.

In a similar vein, Anifowose et al. (2020) reported a flexural strength of 6.96 MPa at 2.5% basalt fibre content. Albeit, they emphasise that placing the fibre only at the tension zone had a better impact on the flexural behaviour than randomly distributing it throughout the concrete mixture. In addition, Li et al. (2022b) also observed significant improvements in flexural strength, crack resistance, and frost resistance in BFRC. The overlap of the percentage error bars in Fig. 5 reveals a non-significant increment in flexural performance with an increase in basalt fibre.

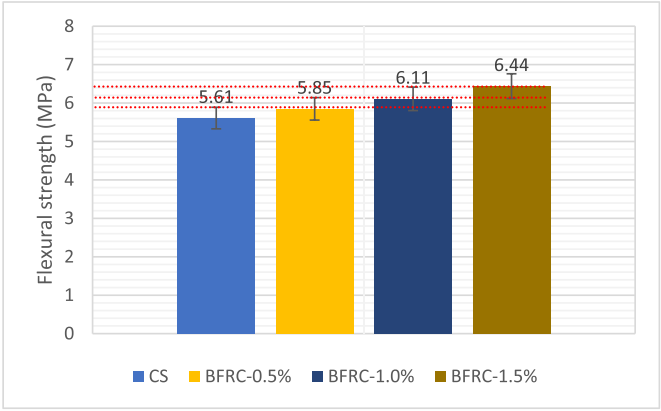

Fig. 6. Average flexural strength of BFRC at 28 days.

4.4.2. Response surface results

In Fig. 8, the flexural performance of concrete samples containing varying fractions of basalt fibre (BF) and silica fume (SF) is compared. The results show a noticeable increase in flexural strength within the ranges of 0.4%–1.5% for BF and 1%–3.5% for SF. The highest value recorded is 9.42 MPa in samples containing 1.5% BF and 0.4% SF, resulting in a significant 46% increase compared to the control sample.

The increased performance can be due to several factors, including increased flexural fracture energy of the concrete, enhanced deflection capability, higher ultimate load, and higher energy absorption rate before rupture resulting from the adequacy and distribution of the fibres which prevent the propagation of micro-cracks thereby prolonging the breaking point of the concrete. It is worth noting, however, that the flexural strength is found to be directly proportional to the BF content and inversely proportional to the SF content. Therefore, further research exploring longer and higher BF content is highly recommended.

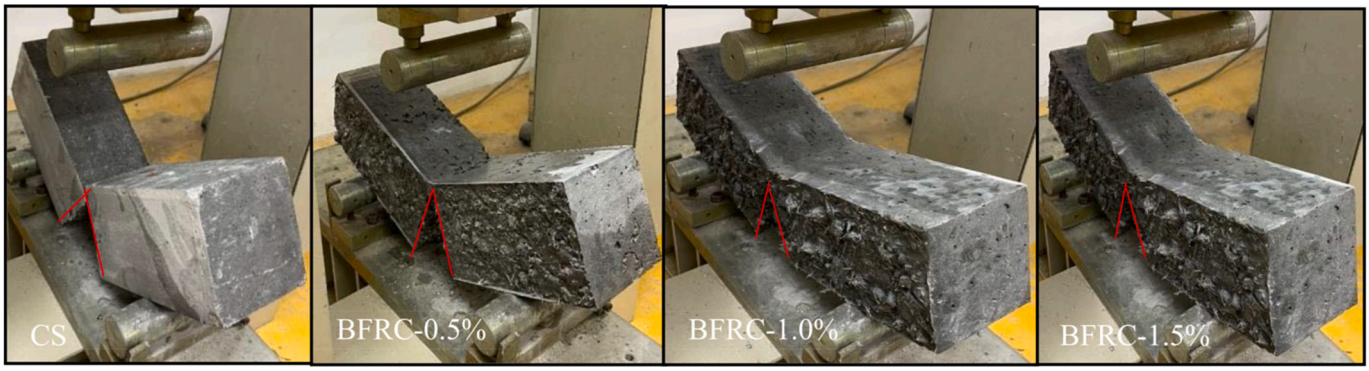

Fig. 7. Comparison of flexural failure modes of samples containing basalt fibre and control sample.

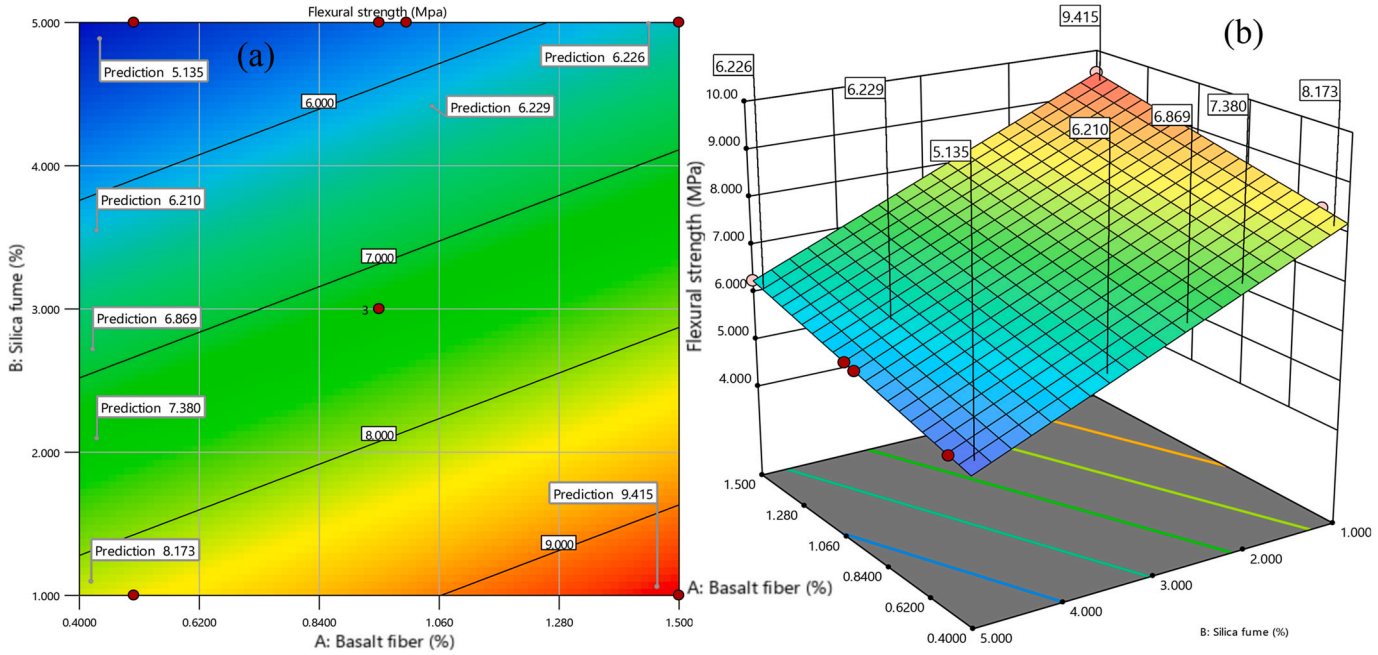

Fig. 8. (a) 2-D contour (b) 3-D response surface representation of the combined influence of Basalt Fiber and Silica Fume on Flexural strength.

4.5. Impact resistance

4.5.1. Experimental results

In comparing the impact resistance of BFRC samples with CS, Fig. 9 reveals a notable improvement in damage resistance. The BFRC samples exhibit increased impact resistance with an increase in basalt fibre content following the same pattern as the flexural strength. Notably, the maximum resistance is observed in BFRC-1.5%.

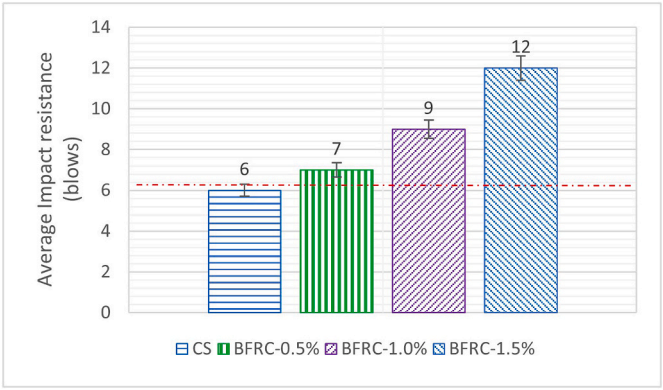

Fig. 9. Average Impact resistance of BFRC at 28 days.

This could be due to improved energy absorption and distribution within the concrete matrix, thereby averting localised energy accumulation. Consequently, the strong interaction between the fibres and matrix effectively transfers the applied force from the concrete matrix to the fibres, resulting in improved impact resistance. A similar trend of improvement in impact resistance with BF was reported by Sateshkumar et al. (2018).

4.5.2. Response surface results

The combined influence of basalt fibre (BF) and silica fume (SF) reveals a complicated, yet interesting relationship as illustrated in Fig. 10 (a) and (b). Close observations indicate that impact resistance is influenced variably by different ranges of BF when SF content is increased. Improvement in the impact resistance is observed in mixes with BF up to 0.84%, with a declining trend in samples containing BF beyond 0.84% and SF between 1% and 3%. Nonetheless, improvement in impact resistance was renewed with increased SF from 3% up to 5%, as represented by increasing contours from 8 to 15 in Fig. 10 (a). The results reveal an impressive relationship for all combined volume ratios, albeit some combinations are non-significant. The highest blows of 13 and 15 are obtained at the lowest (BF 0.4%, SF 1%) and extreme combinations

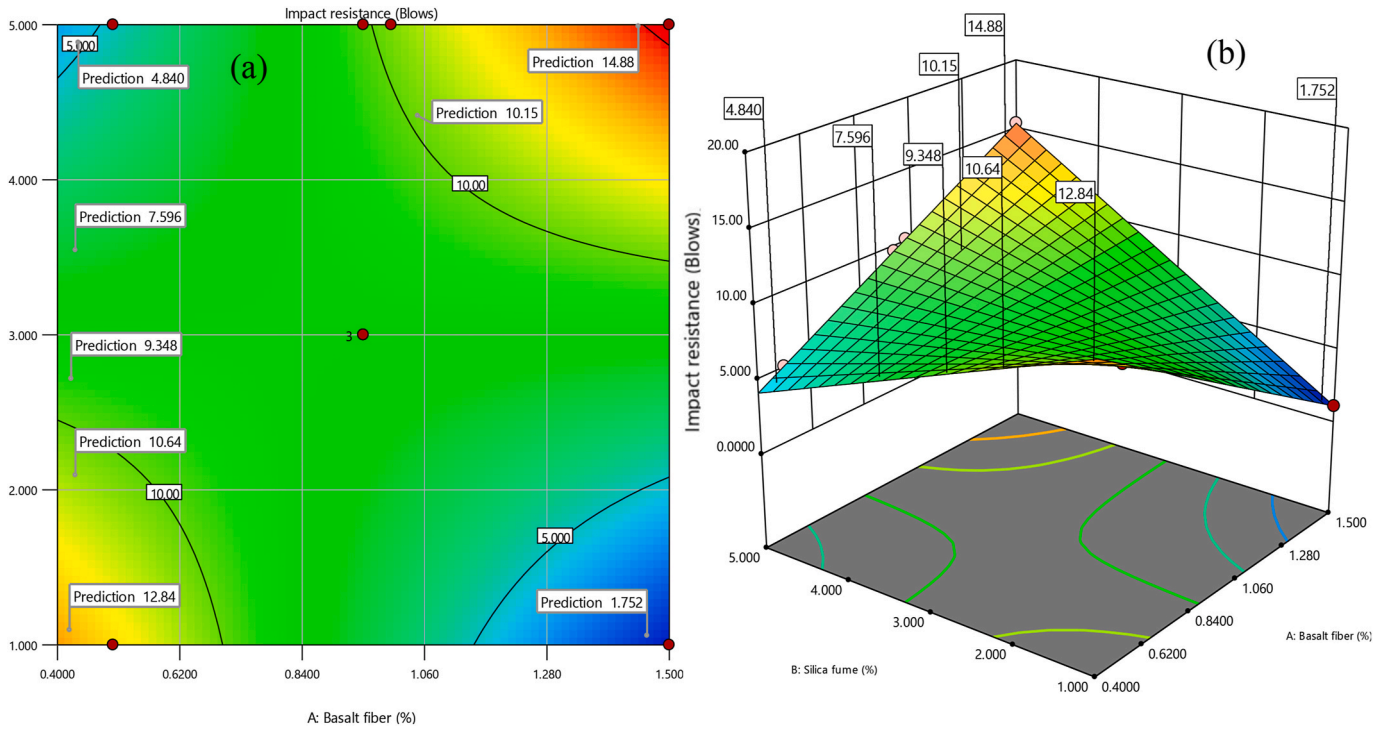

Fig. 10. (a) 2-D contour (b) 3-D response surface representation of the combined influence of Basalt Fiber and Silica Fume on the Impact resistance of concrete.

(BF 1.5%, SF 5%) which represent 117% and 150% in the ability of the concrete to resist sudden forces or impact without cracking when compared with the control sample.

This remarkable improvement is expected, due to the direct correlation that exists between compressive strength and penetration (Dancygier and Yankelevsky, 1996; O'Neil et al., 1999). Thus, a higher compressive strength as presented in section 4.2 indicates more durable and stronger concrete which can indirectly influence the impact resistance. Similar findings have been reported in various studies, including Esaker et al. (2023). This can further be justified by the formation of strong bonding properties within the cementitious matrix, resulting in enhanced stress transmission from the concrete matrix to the fibre. This, in turn, enhances the load-carrying capacity, minimizing fibre sliding or debonding.

The non-linear pattern observed in the impact resistance properties is likely a result of the inconsistent distribution of fibres in the interfacial transition zone (ITZ), which is the area between the aggregate particles and the surrounding cementitious matrix. While there is an overall enhancement in impact resistance, the most significant increase occurs in mixes with lower and higher doses, with the intermediate mixes showing less pronounced effects.

5. Graphical optimization

Fig. 11 (a, b, c and d) illustrates the individual response overlay plots highlighting specific regions where an array of optimal predicted responses can be achieved. In each case, X1 represent Basalt fibre and X2 represents Silica fume, while the yellow region highlights contour(s) where an entire defined factor range can be obtained with a 95% confidence interval. Fig. 11(a) shows the boundaries of compressive strength within 37 MPa–49 MPa, whereas Fig. 11(b), (c) and 11(d) illustrate plots of Split tensile strength, flexural strength and impact resistance within 10 MPa–16 MPa, 7 MPa–9.54 MPa, and 8 blows to 16 blows respectively.

The optimised (maximisation) responses within a 95% confidence interval are presented in Table 6. Moreover, Fig. 12 shows a blend of regions where combined optimal responses can be achieved using optimal volume fraction. Thus, depending on the priority of intent, the individual or combined optimization plot can be utilised. Based on Fig. 12, at an optimal volume fraction of 1.443 and 3.6119, an optimal compressive strength, split tensile strength, flexural strength and impact resistance of 37.18 MPa, 12.58 MPa, 7.33 MPa and 10 blows can be achieved which is equivalent to 30%, 70%, 31%, 67% more than the control sample.

Thus, given the significant improvement, particularly in split tensile and impact resistance, the resulting concrete from the optimised material will be suitable for structures where crack control and structural integrity are crucial. Examples include dams, pavement slabs, and airfield runways that are designed based on bending strength. In addition, the enhanced impact resistance offers a viable alternative to FRP sheets and bars in strengthening concrete that is susceptible to impact loading.

Based on the findings presented, the optimised results for each response reveal a range of basalt fibre and silica fume that offers significant improvement in the mechanical and impact resistance of the concrete. Thus, depending on the specific application, the optimal content can serve as a guide for the appropriate selection of basalt fibre and silica fume.

6. Conclusion

An extensive study on the combined influence of basalt fibre and silica fume is presented using experimental and response surface analysis considering volume fractions of basalt fibre and 1%–5% silica fume. Regression models were developed from experimental data for response prediction purposes. Optimal design technique was used from design expert software for the implementation of the response surface analysis. Based on the findings, the following conclusions are derived.

- Experimental tests alone are not sufficient in fully investigating the influence of more than one factor in a hybrid concrete.
- Incorporating 0.4%–1.5% basalt fibre and 1%–3.5% silica fume has significantly improved the flexural strength of the basalt fibre-reinforced concrete by 11%–46%.

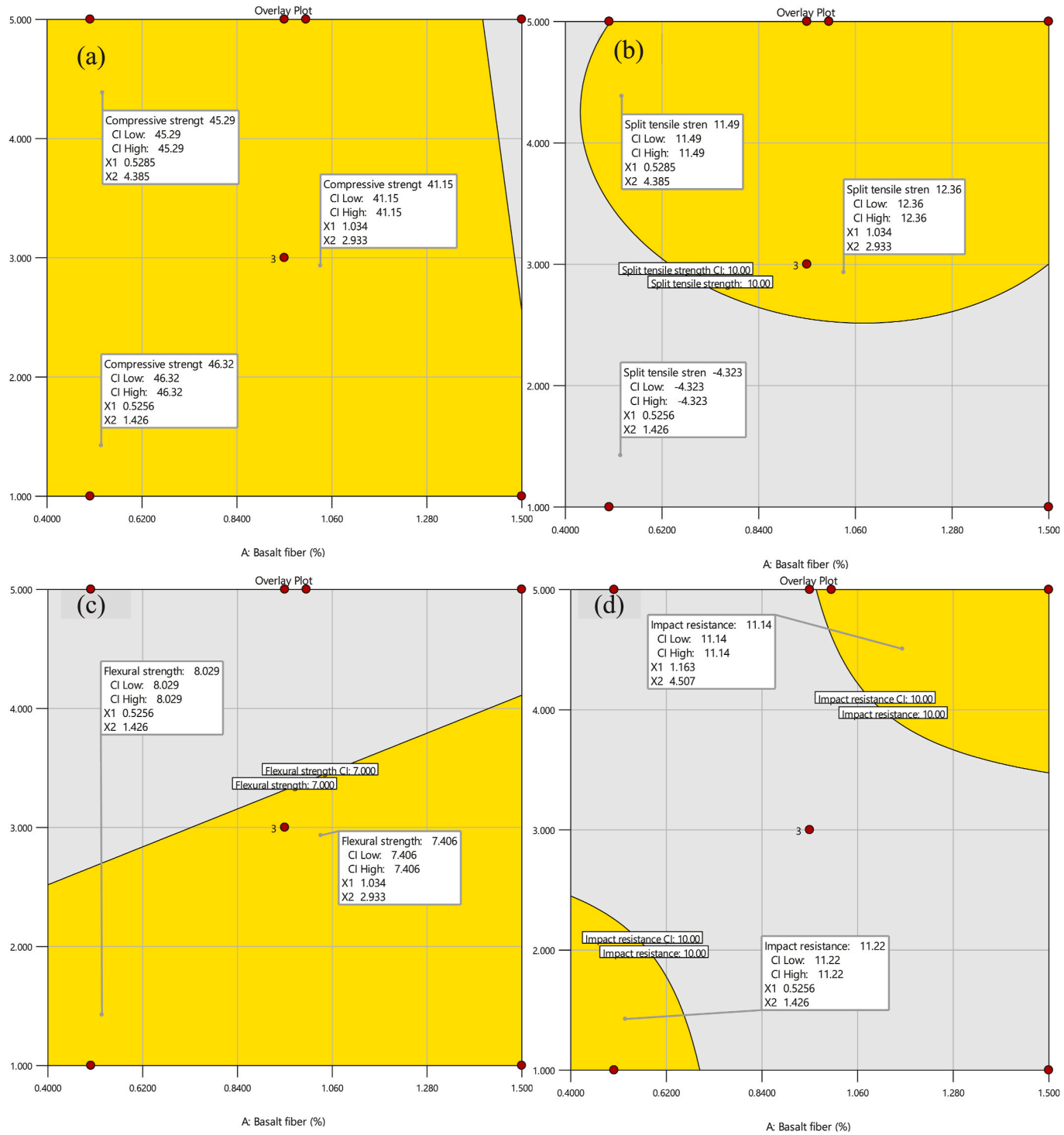

Fig. 11. Overlay plots (a) Compressive Strength (b) Split Tensile Strength (c) Flexural strengths (d) Impact Resistance.

Table 6
Optimised individual responses.

Responses	BF	SF	Optimised values
Compressive strength	0.466	1.3035	46.91
Split tensile strength	1.0517	4.0453	15.33
Flexural Strength	1.3886	1.2751	9.16
Impact resistance	1.4326	4.8045	14

- The BFRC-1.0% concrete showcased higher stiffness in the linear elastic and plastic deformation phases before reaching ultimate stress, while concrete containing 1.5% basalt fibre (BFRC-1.5%) exhibited a higher ultimate stain. Nonetheless, under the same loading condition, the normalised stress ratio indicates a comparable stress-strain response in the ultimate stress region for all the samples.
- The development of tensile strength is directly proportional to the increase in both SF and BF. Improvement in split tensile strength ranging from 35% to 107% was achieved with BF and SF content between 0.4% to 1.5% and 2.5%–5% respectively, with an optimal

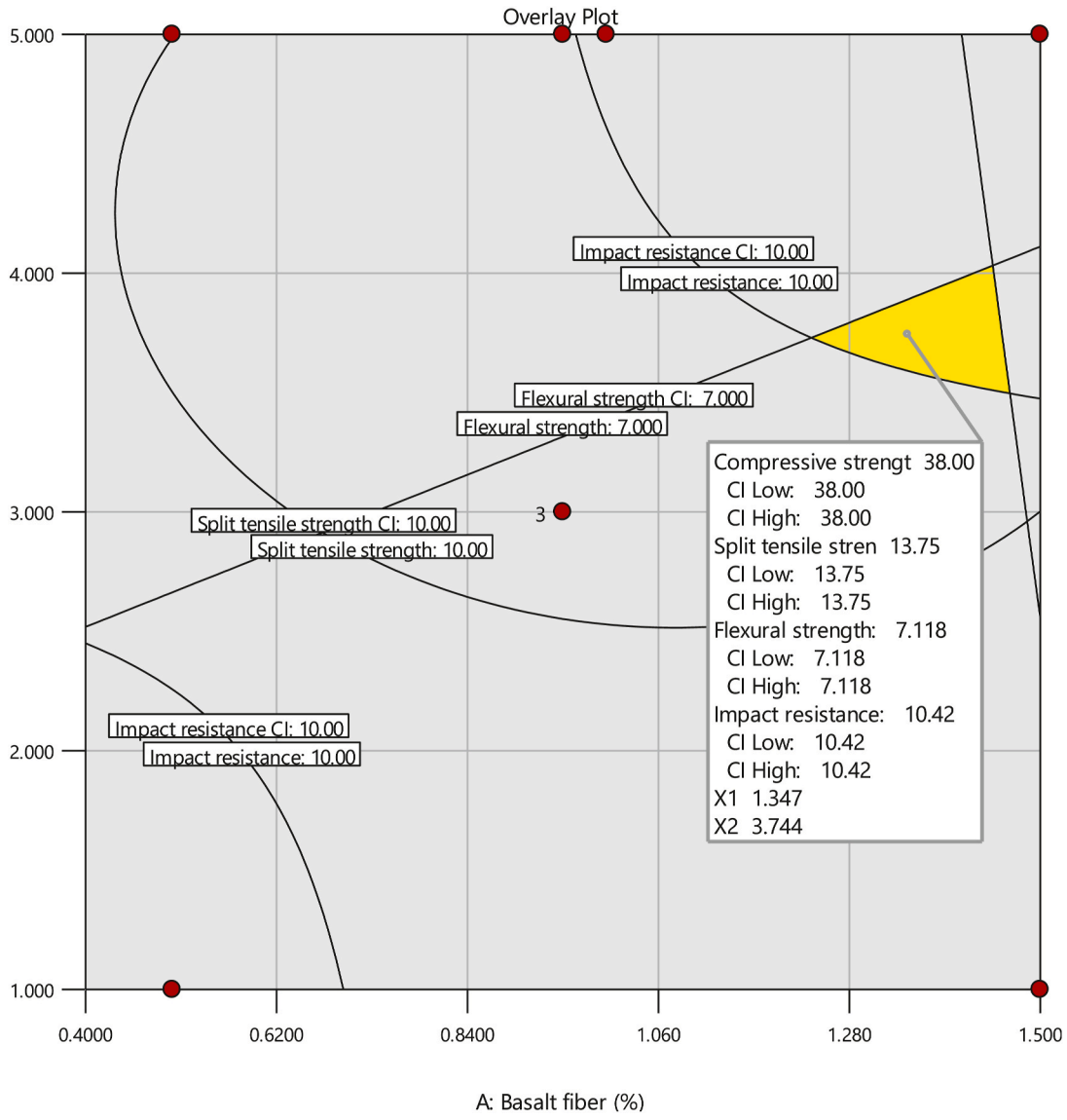

Fig. 12. Graphical optimization plot of combined responses.

BF and SF content of 1% and 4.5% respectively yielding a maximum value of 15.46 MPa.

- Concrete samples containing basalt fibre showed a gradual post-plastic deformation drop in ultimate stress, with higher fibre content leading to a higher ultimate strain, resulting in improved flexural and impact resistance behaviour.
- The impact resistance of concrete reinforced with basalt fibre varies directly proportional to the amount of basalt fibre and inversely proportional to the SF content. The enhanced impact resistance increased up to 67%.
- Improvement of up to 30% in compressive strength, 70% in split tensile strength, 31% in flexural strength, and 67% in impact resistance was achieved with an optimal volume fraction of 1.44% and 3.61% content of BF and SF respectively.

Based on the highlighted conclusions, the inclusion of basalt fibre and silica fume reveals significant enhancement in the mechanical and impact properties of the concrete with an improvement of at least 30% in each response considered.

CRediT authorship contribution statement

Idris Ahmed Ja'e: Writing – review & editing, Writing – original draft, Visualization, Validation, Supervision, Software, Project administration, Formal analysis, Data curation, Conceptualization. **Raja Amirul Naquib bin Raja Sazrin:** Writing – original draft, Investigation, Data curation, Conceptualization. **Agusril Syamsir:** Writing – review & editing, Writing – original draft, Supervision, Methodology, Investigation, Data curation, Conceptualization. **Naraindas Bheel:** Visualization, Software, Investigation, Data curation. **Chiemela Victor Amaechi:** Visualization, Software, Investigation, Data curation. **Teh Hee Min:** Visualization, Software, Investigation, Data curation. **Vivi Anggraini:** Writing – review & editing, Data curation.

Declaration of competing interest

The authors declare that they have no known competing financial interests or personal relationships that could have appeared to influence the work reported in this paper.

Data availability

The authors do not have permission to share data.

Acknowledgement

The authors are grateful to acknowledge the IRMC UNITEN and the Institute of Energy Infrastructure (IEI) for the lab facilities and financial support provided through Bold Publication Fund "J510050002-IC-6 BOLDREFRESH2025—CENTRE OF EXCELLENCE".

References

Abbass, W., Khan, M.I., Mourad, S., 2018. Evaluation of mechanical properties of steel fiber reinforced concrete with different strengths of concrete. Construct. Build. Mater. 168, 556–569.

Abdulkadir, I., Mohammed, B.S., Liew, M., Wahab, M., 2021. Modelling and optimization of the mechanical properties of engineered cementitious composite containing crumb rubber pretreated with graphene oxide using response surface methodology. Construct. Build. Mater. 310, 125259.

Abna, A., Mazloom, M., 2022. Flexural properties of fiber reinforced concrete containing silica fume and nano-silica. Mater. Lett. 316, 132003.

Adesina, A., Bastani, A., Heydariha, J.Z., Das, S., Lawn, D., 2020. Performance of basalt fibre-reinforced concrete for pavement and flooring applications. Innovative Infrastructure Solutions 5, 1–10.

Adil, G., Kevern, J.T., Mann, D., 2020. Influence of silica fume on mechanical and durability of pervious concrete. Construct. Build. Mater. 247, 118453.

Anifowose, P.O., Abubakar, A.F.a., Zhihong, X., 2020. (Year).Effects of basalt fiber length and distribution on flexural strength of cement-based materials. In: International Conference on Urban Engineering and Management Science. ICUEMS), pp. 60–63, 2020: IEEE.

Atea, R.S., 2019. A case study on concrete column strength improvement with different steel fibers and polypropylene fibers. J. Mater. Res. Technol. 8 (6), 6106–6114.

Banthia, N., Sappakittipakorn, M., 2007. Toughness enhancement in steel fiber reinforced concrete through fiber hybridization. Cement Concr. Res. 37 (9), 1366–1372.

Bheel, N., Mohammed, B.S., Ahmed Ali, M.O., Shafiq, N., Mohamed Tag-eldin, E., Ahmad, M., 2023. Effect of polyvinyl alcohol fiber on the mechanical properties and embodied carbon of engineered cementitious composites. Results in Engineering 20, 101458. https://doi.org/10.1016/j.rineng.2023.101458.

Bhonde, V., Fadadu, M., Patel, S., Mungule, M., Iyer, K., Year), 2022. A comparison of stress-strain behaviour of conventional and high strength concrete. ASPS Conference Proceedings 1 (4), 1323–1326.

Dancygier, A., Yankelevsky, D., 1996. High strength concrete response to hard projectile impact. Int. J. Impact Eng. 18 (6), 583–599.

Design Expert Software -v13, 2021 [Online]. Available: https://www.statease.com/docs/v13/contents/analysis/anova-output/.

Dias, D.P., Thaumaturgo, C., 2005. Fracture toughness of geopolymeric concretes reinforced with basalt fibers. Cement Concr. Compos. 27 (1), 49–54. https://doi.org/10.1016/j.cemconcomp.2004.02.044.

E Taha, T., M Tahwia, A., H Abdelraheem, A., 2019. Durability performance of silica fume Self-Compacting Concrete. Engineering Research Journal 164, 193–213.

Emad, W., et al., 2022. (Year).Prediction of concrete materials compressive strength using surrogate models. In: Structures, vol. 46. Elsevier, pp. 1243–1267.

Esaker, M., Thermou, G.E., Neves, L., 2023. Impact resistance of concrete and fibre-reinforced concrete: a review. Int. J. Impact Eng. 180, 104722 https://doi.org/10.1016/j.ijimpeng.2023.104722.

Gencel, O., et al., 2022. Basalt fiber-reinforced foam concrete containing silica fume: an experimental study. Construct. Build. Mater. 326, 126861.

IA, J.E., Sulaiman, T., Abdurrahman, A., 2019. Evaluation of pozzolanic materials and their influence on cement and workability retention of concrete. Nigerian Journal of Scientific Research 18 (4), 329–336.

Jae, I.A., et al., 2023. Experimental and predictive evaluation of mechanical properties kenaf-polypropylene fibre reinforced concrete using response surface methodology. Developments in the Built Environment, 100262. https://doi.org/10.1016/j.dibe.2023.100262.

Khan, M.B., et al., 2023. Optimization of fresh and mechanical characteristics of carbon fiber-reinforced concrete composites using response surface technique. Buildings 13 (4), 852.

Koksal, F., Kocabeyoglu, E.T., Gencel, O., Benli, A., 2021. The effects of high temperature and cooling regimes on the mechanical and durability properties of basalt fiber reinforced mortars with silica fume. Cement Concr. Compos. 121, 104107.

Köksal, F., Beycioğlu, A., Dobiszewska, M., 2022. Optimization based on toughness and splitting tensile strength of steel-fiber-reinforced concrete incorporating silica fume using response surface method. Materials 15 (18), 6218.

Lee, J.-H., Cho, B., Choi, E., 2017. Flexural capacity of fiber reinforced concrete with a consideration of concrete strength and fiber content. Construct. Build. Mater. 138, 222–231.

Li, Y., et al., 2022a. A review on durability of basalt fiber reinforced concrete. Compos. Sci. Technol. 225, 109519.

Li, Z., Shen, A., Chen, Z., Guo, Y., Yang, X., 2022b. Research progress on properties of basalt fiber-reinforced cement concrete. Mater. Today Commun., 104824

Mazloom, M., Mirzamohammadi, S., 2019. Thermal effects on the mechanical properties of cement mortars reinforced with aramid, glass, basalt and polypropylene fibers. Advances in materials research: AMR (Adv. Magn. Reson.) 8 (2), 137–154.

Mazloom, M., Mirzamohammadi, S., 2021. Fracture of fibre-reinforced cementitious composites after exposure to elevated temperatures. Mag. Concr. Res. 73 (14), 701–713.

Mazloom, M., Ramezanianpour, A.A., Brooks, J.J., 2004. Effect of silica fume on mechanical properties of high-strength concrete. Cement Concr. Compos. 26 (4), 347–357. https://doi.org/10.1016/S0958-9465(03)00017-9.

Mazloom, M., Karimpanah, H., Karamloo, M., 2020. Fracture behavior of monotype and hybrid fiber reinforced self-compacting concrete at different temperatures. Advances in Concrete Construction 9 (4), 375.

Özkılıç, Y.O., et al., 2023. Shear performance of reinforced expansive concrete beams utilizing aluminium waste. J. Mater. Res. Technol. 24, 5433–5448.

O'Neil, E.F., Neeley, B.D., Cargile, J.D., 1999. Tensile properties of very-high-strength concrete for penetration-resistant structures. Shock Vib. 6 (5–6), 237–245.

Philip, P.M., Joseph, A., Koshy, R.Z., Jossy, A., 2023. (in press). Mechanical and permeability properties of basalt fibre Reinforced concrete. Mater. Today: Proc. https://doi.org/10.1016/j.matpr.2023.05.133.

Poorarbabi, A., Ghasemi, M., Moghaddam, M.A., 2020. Concrete compressive strength prediction using non-destructive tests through response surface methodology. Ain Shams Eng. J. 11 (4), 939–949.

Sadrmomtazi, A., Tahmouresi, B., Saradar, A., 2018. Effects of silica fume on mechanical strength and microstructure of basalt fiber reinforced cementitious composites (BFRCC). Construct. Build. Mater. 162, 321–333. https://doi.org/10.1016/j.conbuildmat.2017.11.159.

Sarabia, L.A., Ortiz, M.C., 2009. 1.12 - response surface methodology. In: Brown, S.D., Tauler, R., Walczak, B. (Eds.), Comprehensive Chemometrics. Elsevier, Oxford, pp. 345–390.

Saradar, A., Nemati, P., Paskiabi, A.S., Moein, M.M., Moez, H., Vishki, E.H., 2020. Prediction of mechanical properties of lightweight basalt fiber reinforced concrete containing silica fume and fly ash: experimental and numerical assessment. J. Build. Eng. 32, 101732.

Sateshkumar, S.K., Awoyera, P.O., Kandasamy, T., Nagaraj, S., Murugesan, P., Ponnusamy, B., 2018. Impact resistance of high strength chopped basalt fibre-reinforced concrete. Revista de la Construcción. Journal of Construction 17 (2), 240–249.

Scalici, T., Pitarresi, G., Badagliacco, D., Fiore, V., Valenza, A., 2016. Mechanical properties of basalt fiber reinforced composites manufactured with different vacuum assisted impregnation techniques. Compos. B Eng. 104, 35–43.

Sulaiman, T.A., Ja'e, I.A., Yau, Y., Hashim, Y.M., 2020. Investigation of crumb rubber proportion on compressive strength and water absorption of crumb rubber mortar. ATBU Journal of Science, Technology and Education 8 (2), 84–91.

Tahwia, A.M., Helal, K.A., Youssf, O., 2023. Chopped basalt fiber-reinforced high-performance concrete: an experimental and analytical study. Journal of Composites Science 7 (6), 250.

Wu, H., Qin, X., Huang, X., Kaewunruen, S., 2023. Engineering, mechanical and dynamic properties of basalt fiber reinforced concrete. Materials 16 (2), 623.

Xie, L., Sun, X., Yu, Z., Zhang, J., Li, G., Diao, M., 2023. Experimental study and mechanism analysis of the shear dynamic performance of basalt fiber–reinforced concrete. J. Mater. Civ. Eng. 35 (1), 04022374.

Xue, Z., Qi, P., Yan, Z., Pei, Q., Zhong, J., Zhan, Q., 2023. Mechanical properties and crack resistance of basalt fiber self-compacting high strength concrete: an experimental study. Materials 16 (12), 4374.

Zhang, G., et al., 2022. Properties of sustainable self-compacting concrete containing activated jute fiber and waste mineral powders. J. Mater. Res. Technol. 19, 1740–1758.

Zielinski, K., Olszewski, P., 2005. Untersuchungen zu Basaltfasern als Faserbewehrung: der Einfluss von Basaltfasern auf ausgewählte physische und mechanische Eigenschaften von Zementmörtel. Betonw. Fertigtl. 71 (3), 28–33.